



CHORUS

This is the accepted manuscript made available via CHORUS. The article has been published as:

Laser Hosing in Relativistically Hot Plasmas

G. Li, W. B. Mori, and C. Ren

Phys. Rev. Lett. **110**, 155002 — Published 9 April 2013

DOI: [10.1103/PhysRevLett.110.155002](https://doi.org/10.1103/PhysRevLett.110.155002)

Laser hosing in relativistically hot plasmas

G. Li[†], W. B. Mori[§], and C. Ren^{†‡}

[†]*Department of Mechanical Engineering and Laboratory for Laser Energetics,*

[‡]*Department of Physics and Astronomy,*

University of Rochester, Rochester, NY 14627 and

[§]*Departments of Physics & Astronomy and Electrical Engineering,*

University of California, Los Angeles, CA 90095

Abstract

Electron response in an intense laser is studied in the regime where the electron temperature is relativistic. Equations for laser envelope and plasma density evolution, both in the electron plasma wave and ion acoustic wave regimes, are re-derived from the relativistic fluid equations to include relativistic plasma temperature effect. These equations are used to study short-pulse and long-pulse laser hosing instabilities using a variational method approach. The analysis shows that relativistic electron temperatures reduce the hosing growth rates and shift the fastest-growing modes to longer wavelengths. These results resolve a long-standing discrepancy between previous non-relativistic theory and simulations/experiments on hosing.

Previous studies in intense short-pulse laser-plasma interactions discovered many interesting phenomena rooted in relativistic electron oscillation velocities, including relativistic self-focusing[1, 2], ponderomotive plasma blowout[2, 3], and mutual interactions between laser beams in a plasma[4, 5]. Analyses of these phenomena assumed electrons' thermal energy small compared to their oscillation energy and adopted a cold plasma approach. Recently-available kJ-class short-pulse lasers have not only the intensity to make electrons oscillate at relativistic speeds but also the energy to heat these electrons to relativistic temperatures. In recent Particle-in-Cell (PIC) simulations of kJ-class laser channeling in mm-scale underdense plasmas for fast ignition the residual electron temperature T_e in the channel was found to be multi-MeV [6, 7]. Relativistic T_e was also observed in PIC simulations with sub-ps intense pulses of energy as low as 10J[3]. Relativistic T_e can reduce the electron oscillation velocity and decouple the laser from the plasma[3, 6, 7]. However, how relativistic T_e affects a wide range of plasma optical phenomena in intense laser-plasma interactions remains largely unexplored.

In this Letter, we will show that relativistic T_e can significantly affect laser hosing[8–12], an instability important to both laser wake field accelerators (LWFA) [13] and fast ignition (FI) [14]. Hosing affects laser propagation and wake field generation in LWFA. LWFA-relevant hosing is in the short-pulse regime, mediated by electron plasma waves[8–11]. In the channeling/hole-boring scheme of FI, the channeling pulse can also suffer hosing instability, causing channel bending and bifurcation [6, 7]. Hosing in this long-pulse regime involves ion motion and is mediated by the ion acoustic waves[12]. However, there is a long-standing discrepancy on the wavelengths of the dominant hosing modes between the existing theory and PIC simulations/experiments. In the short-pulse regime, the hosing modes observed in the PIC simulations [10] had wavelengths 2-10 times longer than that predicted by the cold plasma theory [8, 9] for the fastest-growing mode. The predicted fastest-growing mode at the plasma wavelength was never observed in the simulations. The lack of such modes was attributed to the interference of Raman instabilities and the suppression of the plasma wave due to plasma heating [10] but no quantitative theory was given. In one reported experimental observation of laser hosing [15], the observed hosing wavelengths were also much longer than predicted by the short-pulse theory. The discrepancy was speculated due to ion motion. As will be shown in this Letter, long-pulse hosing theory including the ion motion but assuming a non-relativistic T_e still predicts a fastest-growing mode at a

much shorter wavelength than observed. Similar discrepancy also exists between the theory and the channeling simulations[6, 7]. In addition, some hosing-like structures observed in laser-plasma experiments, also with wavelengths longer than what predicted by the existing theory, were attributed to surface waves [16] or asymmetry laser transverse profile [17].

The discrepancies between the predicted and observed hosing wavelengths can be resolved by properly treating the electron temperature effects in the relativistic regime. From the full relativistic fluid theory, we will re-derive the coupled equations of laser envelope and plasma density in the relativistic T_e regime. Analyses of these equations using a variational method show that as T_e becomes relativistic the dominant hosing modes shift to longer wavelengths for both short- and long-pulse modes, agreeing with the experiments and PIC simulations. The derived equations also lay the basis for studying other nonlinear plasma optical phenomena in the relativistic T_e regime[18, 19].

From the relativistic Vlasov equation a fully relativistic fluid theory had been developed[20, 21]. Here we restrict ourselves to a locally isotropic particle distribution f . The resultant pressure tensor $\Theta^{ij} = m \int f(U^i - \langle U^i \rangle)(U^j - \langle U^j \rangle)/\gamma d^3U$ is diagonal with $\Theta^{11} = \Theta^{22} = \Theta^{33} \equiv p$. Here U^i ($i = 1, 2, 3$) are the components of the momentum (per unit mass) vector \mathbf{U} , $\gamma = \sqrt{1 + \mathbf{U} \cdot \mathbf{U}/c^2}$, c the speed of light, m the particle mass, and $\langle \mathbf{U} \rangle$ is the fluid momentum, $\langle U^i \rangle = (\int f U^i / \gamma d^3U) / (\int f / \gamma d^3U)$.

For the locally isotropic f , the relativistic fluid momentum equation [Eq. (85) in Ref.[21]] can be written as

$$mn\left(\frac{\partial}{\partial t} + \mathbf{v} \cdot \nabla\right)[\Gamma\alpha\mathbf{v}] = n\mathbf{F} - \nabla p, \quad (1)$$

where \mathbf{v} is the fluid velocity, $\Gamma = 1/\sqrt{1 - \mathbf{v} \cdot \mathbf{v}/c^2}$ is the relativistic factor from the fluid velocity, $n = \int f d^3U$ is the particle density, and $\mathbf{F} = q(\mathbf{E} + \mathbf{v} \times \mathbf{B}/c)$ is the Lorentz force per particle. The thermal parameter α represents relativistic mass increase from the random motion of the particles and is defined as $\alpha = (p + \bar{e})/(\bar{n}mc^2)$, where $\bar{e} = mc^2 \int \bar{\gamma} f d^3\bar{U}$ is the internal energy density in the local rest frame (which moves relative to the lab frame with \mathbf{v}) and $\bar{n} = n/\Gamma$ is the particle density in the local rest frame. Different but equivalent forms of Eq. (1) have also been derived based on the invariance of the momentum-energy tensor [3, 22, 23]. Equation 1 shows that the total relativistic factor of a fluid element is $\Gamma\alpha$.

For a cold species, $p = 0$, $\bar{e} = \bar{n}mc^2$ and $\alpha = 1$. As the particles become hotter α increases, but significant deviation from 1 occurs only when the particles are relativistically hot. In

Figure 1 α 's from two common distributions are plotted. One is from a non-relativistic Maxwellian distribution $f_M = \bar{n}(2\pi U_{th}^2)^{-3/2} \exp(-U^2/2U_{th}^2)$ and the other is from a relativistic Maxwell-Juttner distribution $f_{MJ} = \bar{n}[4\pi c U_{th}^2 K(2, c^2/U_{th}^2)]^{-1} \exp(-c\sqrt{c^2 + U^2}/U_{th}^2)$, where K is the modified Bessel function of the second kind. For same U_{th} , f_{MJ} gives a much larger α than f_M when $U_{th}/c > 1$. For the Maxwell-Juttner distribution, when $U_{th}/c = 1$, the thermal energy $\bar{e} - \bar{n}mc^2 = 1.2$ MeV and $\alpha = 4.4$ for electrons. For ions, $\alpha = 1$ is a good approximation for sub-GeV thermal energies.

As an initial study on laser propagation in a relativistically hot plasma we focus on the simple case of a uniform and constant α . The high frequency electron quiver velocity in the laser field can be found from Eq. 1[3], $\mathbf{v}_{os}/c \approx \mathbf{a}/(\alpha\Gamma)$, where $\mathbf{a} = e\mathbf{A}/m_e c^2$ is the normalized laser vector potential. For weakly nonlinear cases with $|\mathbf{a}| < 1$ or relativistically hot electrons with $|\mathbf{a}| > 1$ but $|\mathbf{a}|/\alpha < 1$, the time-averaged fluid Γ can be approximated as $\Gamma \approx 1 + a^2/(4\alpha^2)$, where a is the envelope of \mathbf{a} . Under these approximations the widely-used laser envelope equation[24] becomes

$$(c^2\nabla_{\perp}^2 + 2ik_L c \frac{\partial}{\partial \tau} + 2\frac{\partial^2}{\partial \psi \partial \tau})a = \omega_{p0}^2(1 + \delta n - \frac{|a|^2}{4\alpha^2})\frac{a}{\alpha}, \quad (2)$$

in terms of the "speed of light variables" $\tau = x/c$ and $\psi = t - x/c$. Here k_L is the laser wavenumber, $\delta n = n/n_0 - 1$ is the normalized electron density change and $\omega_{p0} = (4\pi n_0 e^2/m_e)^{1/2}$ is the plasma frequency.

In the short-pulse regime, the equation for δn [24] becomes [25],

$$(\alpha\frac{\partial^2}{\partial \psi^2} + \omega_{p0}^2 - \frac{\gamma_p T_e}{m_e} \nabla^2)\delta n = \frac{c^2}{\alpha} \nabla^2 \frac{|a|^2}{4}. \quad (3)$$

Here, $T_e \equiv m_e U_{th}^2$ is the electron temperature and the adiabatic constant $\gamma_p = 5/3$ is the same as in the non-relativistic case. In the long pulse regime, δn follows the ion density perturbation described by the ion acoustic equation[12], which becomes [25]

$$(\frac{\partial^2}{\partial \psi^2} - C_s^2 \nabla^2)\delta n = \frac{Z m_e c^2}{m_i \alpha} \nabla^2 \frac{|a|^2}{4}, \quad (4)$$

where $C_s = \sqrt{(ZT_e + T_i)/m_i}$ is the ion sound speed. Setting $\alpha = 1$, Eqs.2-4 recover the usual non-relativistic equations that were widely used in the study of nonlinear plasma optics [12, 24]. With α , they are for the first time extended to the regime of relativistic T_e .

We now show how the dominant hosing modes change as α increases. We use a variational method [12, 26, 27] to derive dispersion relations of hosing instabilities from the relevant

equations. For the $\alpha = 1$ case, Duda et al. demonstrated the feasibility of the variational approach for short-pulse hosing, including the dispersive term (the mixed derivative term in Eq.2) [27], and long-pulse hosing without the dispersive term [12]. We have extended the analysis to $\alpha > 1$.

We start with the long pulse hosing. Typical hosing wavenumbers in this regime are expected to be $k \sim \omega_{pi}/c$ where ω_{pi} is the ion plasma frequency $\omega_{pi} = \sqrt{4\pi ne^2/m_i}$. For typical laser and plasma parameters in, for example, laser channeling in fast ignition[6, 7], longitudinal variation is much smaller than transverse variations and ∇^2 can be approximated by ∇_{\perp}^2 in Eqs. 2 and 4. Also the dispersive term in Eq. 2 can be neglected, which has been confirmed by analysis including this term [25]. To find a Lagrangian density L for which the Euler-Lagrangian equations when varying the action $S = \int dydzd\psi d\tau L$ are Eqs. (2) and (4), we introduce a new potential ϕ [12], $\nabla_{\perp}^2 \phi = 1 + \delta n$. The envelope and density equations written in ϕ and a are now

$$(\nabla_{\perp}^2 + 2i\hat{k}_L \frac{\partial}{\partial \hat{\tau}} - \frac{1}{\alpha} \nabla_{\perp}^2 \phi + \frac{|a|^2}{4\alpha^3})a = 0, \quad (5)$$

$$\nabla_{\perp}^2 [(\frac{\partial^2}{\partial \hat{\psi}^2} - c_s^2 \nabla_{\perp}^2)\phi - \frac{Zm_e}{m_i} \frac{|a|^2}{4\alpha}] = 0, \quad (6)$$

where the quantities with a caret are space and time scales normalized to c/ω_{p0} or $1/\omega_{p0}$ and c_s is C_s normalized to c . The Lagrangian density then is

$$L = \frac{Zm_e}{m_i} [\nabla_{\perp} a \nabla_{\perp} a^* + i\hat{k}_L (a \partial_{\hat{\tau}} a^* - a^* \partial_{\hat{\tau}} a) - \frac{1}{\alpha} \nabla_{\perp} |a|^2 \nabla_{\perp} \phi - \frac{|a|^4}{8\alpha^3}] - 2(\nabla_{\perp} \partial_{\hat{\psi}} \phi)^2 + 2c_s^2 (\nabla_{\perp}^2 \phi)^2, \quad (7)$$

which recovers Eqs. (5) and (6) if varying with respect to a , a^* and ϕ . Gaussian trial functions are chosen for a and ϕ ,

$$a = a_0 e^{i\chi} e^{ik_y \tilde{y}_a} e^{ik_z \tilde{z}_a} e^{-[1-i\alpha_y] \tilde{y}_a^2 / w_{ya}^2} e^{-[1-i\alpha_z] \tilde{z}_a^2 / w_{za}^2}, \quad (8)$$

$$\phi = \Phi e^{-2[\tilde{y}_\phi^2 / w_{y\phi}^2 + \tilde{z}_\phi^2 / w_{z\phi}^2]}. \quad (9)$$

Here, $\tilde{y}_a = y - y_a(\hat{\psi}, \hat{\tau})$ and $\tilde{y}_\phi = y - y_\phi(\hat{\psi}, \hat{\tau})$, where y_a and y_ϕ are the centroids of a and ϕ respectively; $a_0 e^{i\chi}$ is the complex amplitude of a and Φ is the amplitude of ϕ ; w_{ya} and $w_{y\phi}$ are the spot sizes of a and ϕ respectively; k_y and α_y are the wavenumber and wave front curvature of a respectively. The quantities \tilde{z}_a , \tilde{z}_ϕ , w_{za} , $w_{z\phi}$, k_z and α_z are similarly defined. All these parameters are functions of $\hat{\psi}$ and $\hat{\tau}$. Substituting the trial functions into Eq. (7)

and performing the integration over y and z yield a reduced Lagrangian density, for which the Euler-Lagrangian equations are a set of equations for the trial function parameters. A matched beam equilibrium solution ($\partial_{\hat{\tau}} = 0$), where the laser spot sizes remain constant and the centroids remain straight ($y_a = y_\phi = 0$ and $z_a = z_\phi = 0$), can be found. Perturbing this equilibrium yields the hosing equation (the derivations are similar to those in [27])

$$\partial_{\hat{\tau}}^2 y_{a1} + \Omega_1 y_{a1} = \Omega_1 y_{\phi 1}, \quad (10)$$

$$\partial_{\hat{\psi}}^2 y_{\phi 1} + \Omega_2 y_{\phi 1} = \Omega_2 y_{a1}, \quad (11)$$

where

$$\Omega_1 = \frac{27}{256} \frac{Zm_e}{m_i} \frac{P_0}{\alpha^2 c_s^2 \hat{k}_L^2 \hat{w}_0^4}, \Omega_2 = 4 \frac{c_s^2}{\hat{w}_0^2}. \quad (12)$$

Here $P_0 = a_0^2 \hat{w}_0^2$ is the dimensionless laser power and \hat{w}_0 the normalized spot size. The centroid equations of z_{a1} and $z_{\phi 1}$ are similar to Eq. (10) and (11), with y changed to z . The motions of the centroids in y and z are not coupled.

Assuming $(y_{a1}, y_{\phi 1}) \sim e^{i(\hat{k}\hat{x} - \hat{\omega}\hat{t})}$, a dispersion relation is obtained from Eqs. (10) and (11)

$$\hat{\omega}^4 - 2\hat{k}\hat{\omega}^3 + (\hat{k}^2 - \Omega_1 - \Omega_2)\hat{\omega}^2 + 2\Omega_2\hat{k}\hat{\omega} - \Omega_2\hat{k}^2 = 0. \quad (13)$$

Here, \hat{k} is real and $\hat{\omega}$ is complex, and hosing growth rates are the imaginary part of $\hat{\omega}$.

Figure 2(a) plots growth rates vs. \hat{k} from Eq. 13 for a case of $a_0 = 0.53$, $\hat{w}_0 = 9$, $\hat{k}_L = 10$, $c_s = 0.02$. For a laser of $1\mu m$ -wavelength in a DT-plasma ($Zm_e/m_i = 1/4590$), they correspond to a laser intensity of 0.4×10^{18} W/cm² and a plasma with $n = 10^{19}$ cm⁻³ and $T_e = 1$ MeV, which gives $\alpha = 8.17$ (for f_{MJ}). Comparing with the $\alpha = 1$ case, a relativistic T_e significantly reduces hosing growth rates and also shifts the fastest-growing mode to a longer wavelength. Figure 2(b) plots the wavenumber \hat{k}_M and growth rate $\hat{\gamma}_M$ of the fastest growing mode as a function of T_e , with α calculated from f_{MJ} . It shows that \hat{k}_M first decreases steeply and then increases slowly as T_e increases. And $\hat{\gamma}_M$ first increases, due to the increase of the plasma pressure, and then decreases due to the relativistic effects. Analysis of Eq. 13 shows that the growth rate peaks when $\hat{k}^2 \approx \Omega_1 + \Omega_2$. For non-relativistic T_e , c_s is very small and $\Omega_1 \gg \Omega_2$ (see Eq.12). In this limit \hat{k}_M and $\hat{\gamma}_M$ are $\hat{k}_M^{(lc)} = \sqrt{(27/256)(Zm_e/m_i)a_0}/(\alpha c_s \hat{k}_L \hat{w}_0)$, $\hat{\gamma}_M^{(lc)} = (0.75/\hat{w}_0)(Zm_e/m_i)^{1/6}[c_s a_0/(\alpha \hat{k}_L)]^{1/3}$. Eventually the increase of α saturates $\hat{\gamma}_M^{(lc)}$. For a relativistically hot plasma, c_s and α increase so that

$\Omega_1 \ll \Omega_2$. In this limit \hat{k}_M and $\hat{\gamma}_M$ are

$$\hat{k}_M^{(lh)} \approx \sqrt{\Omega_2} = 2 \frac{c_s}{\hat{w}_0}, \quad (14)$$

$$\hat{\gamma}_M^{(lh)} = \frac{\sqrt{3}}{2} \left(\frac{\Omega_1}{2}\right)^{\frac{1}{3}} \Omega_2^{\frac{1}{6}} = \frac{0.41}{\hat{w}_0} \left(\frac{Zm_e}{m_i}\right)^{\frac{1}{3}} \left(\frac{a_0^2}{c_s \alpha^2 \hat{k}_L^2}\right)^{\frac{1}{3}}. \quad (15)$$

These asymptotic expressions fit well with the numerical solution in Fig. 2(b).

For short-pulse hosing, the density equation Eq.3 has a new electron pressure term $(\gamma_p T_e / m_e) \nabla^2 \delta n$ compared to the previous work [27]. Analysis [25] shows that the ∇_{\perp}^2 part of this term gives only a small correction for the usual case of $\hat{w}_0 > 1$. The ∇_{\parallel}^2 part poses a difficulty for the variational analysis. Here we study the regime of $\alpha \gg \gamma_p T_e / m_e c^2$, which is fully met in a cold or warm plasma and is approximately met in a relativistically hot plasma, to focus on the effects of $\alpha > 1$. In addition, the dispersive term in Eq. 2 mainly reduces the growth rates of the small- k modes and does not affect the k of the dominant mode [25]. Here, we present the non-dispersive case. Introducing a new potential $\phi = |a|^2 / 4\alpha^2 - \delta n$ leads to a Lagrangian density of $L = (1/\alpha)[\nabla_{\perp} a \nabla_{\perp} a^* + i \hat{k}_L (a \partial_{\hat{\tau}} a^* - a^* \partial_{\hat{\tau}} a) - \phi |a|^2 / \alpha + |a|^2 / \alpha] - 2\alpha (\partial_{\hat{\psi}} \phi)^2 + 2\phi^2$. With Gaussian trial functions in Eqs. 8 and 9, a variational analysis leads to a set of equations that are identical to Eqs. 10 and 11 with $\Omega_{1,2}$ replaced by $\Omega_1^{(sp)} = P_0 / (8\alpha^3 \hat{k}_L^2 \hat{w}_0^4)$ and $\Omega_2^{(sp)} = 1/\alpha$. The dispersion relation has the same form as Eq. 13. Typical $\hat{\gamma}$ - \hat{k} curves, as shown in Fig. 2(c) for a case in Ref.[10] with $a_0 = 2$, $\hat{w}_0 = 15$, $\hat{k}_L = 8.5$, show the existence of long wavelength modes [27] but also the shift of the dominant mode to longer wavelengths. In general, $\Omega_1^{(sp)} / \Omega_2^{(sp)} = a_0^2 / (8\alpha^2 \hat{k}_L^2 \hat{w}_0^2) \ll 1$, except for extremely high laser intensities or small spot sizes. Therefore, similar to Eqs.14-15,

$$\hat{k}_M^{(sp)} \approx \frac{1}{\sqrt{\alpha}}, \quad (16)$$

$$\hat{\gamma}_M^{(sp)} = \frac{0.34}{\alpha^{\frac{7}{6}}} \left(\frac{a_0}{\hat{k}_L \hat{w}_0}\right)^{\frac{2}{3}}. \quad (17)$$

The α -dependence clearly show that $\hat{k}_M^{(sp)}$ and $\hat{\gamma}_M^{(sp)}$ decrease as T_e increases. The analytical results of Eqs.16-17 agree well with the full numerical solution of Eq.13 [Fig. 2(d)]. When $T_e = 1$ MeV, the dominant hosing wavelength increases to approximately 3 times of the plasma wavelength.

In one experimental observation of laser hosing by Najmudin *et al* [15], all observed hosing instability fell in a long wavelength region, with no hosing structures of wavelengths shorter

than 200 μm observed. Figure 3(a) shows that for the experimental parameters $a_0 = 2.68$, $w_0 = 8.7 \mu\text{m}$, $n_e = 2.3 \times 10^{19} / \text{cm}^3$ and $Zm_e/m_i = 1/3672$, the maximum growth from the long-pulse hosing theory occurs at $\lambda_h = 30 \mu\text{m}$ for $T_e = 1 \text{ keV}$. The theory predicts that the maximum growth occurs at $\lambda_h = 287 \mu\text{m}$ and $1044 \mu\text{m}$ for $T_e = 100 \text{ keV}$ and 1 MeV respectively. This clearly indicates the importance of plasma heating. Recent 3D PIC simulations of laser channeling observed hosing simultaneously in the two transverse directions[7]. In one simulation, a laser with an initial $a_0 = 2.68$ and $w_0 = 90/k_L$ propagated in a DT-plasma with an exponentially rising density profile of $n_0 = 0.1 - 0.3n_c$. The channeling process was dynamic, including laser self-focusing and significant plasma density modification. The electrons were heated from an initial $T_e = 1 \text{ keV}$ to a final $T_e \approx 6.5 \text{ MeV}$. The hosing growth rates of the dominant mode in the simulation are measured and plotted together with the long-pulse theoretical curves in Figure 3(b). The theoretical curves are calculated for two T_e 's, 100 keV and 1 MeV, with constant parameters of $n_0 = 0.2n_c$, $a_0 = 5.36$, $w_0 = 45/k_L$, accounting for laser self-focusing. Given the differences between the simulation and the theory, the agreement is reasonable. The biggest limitation of Eqs.2-4 is the static α used, in contrast to the dynamic heating processes in the experiments and simulations. To better predict experiments/simulations requires a theory for the laser heating process (how α changes with time), which requires future research.

This work was supported by U.S. Department of Energy under Grants Nos. DE-FG02-06ER54879, DE-FC02-04ER54789, DE-FG52-06NA26195, and DE-FG02-03ER54271. The simulations used resources of the National Energy Research Scientific Computing Center.

-
- [1] C. E. Max, J. Arons, and A. B. Langdon, *Phys. Rev. Lett.* **33**, 209 (1974)
 - [2] G. Z. Sun, E. Ott, Y. C. Lee, and P. Guzdar, *Phys. Fluids* **30**, 526 (1987)
 - [3] K. C. Tzeng and W. B. Mori, *Phys. Rev. Lett.* **81**, 104 (1998)
 - [4] C. Ren, R. G. Hemker, R. A. Fonseca, B. J. Duda, and W. B. Mori, *Phys. Rev. Lett.* **85**, 2124 (2000)
 - [5] C. Ren, B. J. Duda, R. G. Evans, R. A. Fonseca, R. G. Hemker, and W. B. Mori, *Phys. Plasmas* **9**, 2354 (2002)
 - [6] G. Li, R. Yan, C. Ren, T.-L. Wang, J. Tonge, and W. B. Mori, *Phys. Rev. Lett.* **100**, 125002

- (2008)
- [7] G. Li, R. Yan, C. Ren, J. Tonge, and W. B. Mori, *Phys. Plasmas* **18**, 042703 (2011)
 - [8] G. Shvets and J. S. Wurtele, *Phys. Rev. Lett.* **73**, 3540 (1994)
 - [9] P. Sprangle, J. Krall, and E. Esarey, *Phys. Rev. Lett.* **73**, 3544 (1994)
 - [10] B. J. Duda, R. G. Hemker, K. C. Tzeng, and W. B. Mori, *Phys. Rev. Lett.* **83**, 1978 (1999)
 - [11] C. Ren and W. B. Mori, *Phys. Plasmas* **8**, 3118 (2001)
 - [12] B. J. Duda, PhD Thesis, UCLA (2000)
 - [13] T. Tajima and J.M. Dawson *Phys. Rev. Lett.* **43**, 267 (1979)
 - [14] M. Tabak et al., *Phys. Plasma* **1**, 1626 (1994)
 - [15] Z. Najmudin, K. Krushelnick, M. Tatarakis, E. L. Clark, C. N. Danson, V. Malka, D. Neely, M. I. K. Santala, and A. E. Dangor, *Phys. Plasmas* **10**, 438 (2003)
 - [16] L. Willingale, P. M. Nilson, A. G. R. Thomas, J. Cobble, R. S. Craxton, A. Maksimchuk, P. A. Norreys, T. C. Sangster, R. H. H. Scott, C. Stoeckl, C. Zulick, and K. Krushelnick, *Phys. Rev. Lett.* **106** 105002 (2011)
 - [17] M. C. Kaluza, S. P. D. Mangles, A. G. R. Thomas, Z. Najmudin, A. E. Dangor, C. D. Murphy, J. L. Collier, E. J. Divall, P. S. Foster, C. J. Hooker, A. J. Langley, J. Smith, and K. Krushelnick, *Phys. Rev. Lett.* **105** 095003 (2010)
 - [18] S. Guerin, G. Laval, P. Mora, J. C. Adam, and A. Heron, *Phys. Plasmas* **2**, 2807 (1995)
 - [19] Z.-M. Sheng, K. Mima, Y. Sentoku, and K. Nishihara, *Phys. Rev. E* **61**, 4362 (2000)
 - [20] W. A. Newcomb, *Phys. Fluids* **25**, 846 (1982)
 - [21] J. G. Siambis, *Phys. Fluids* **30**, 896 (1987)
 - [22] S. Weinberg, *Gravitation and cosmology*, Wiley (1972)
 - [23] T. Katsouleas and W. B. Mori, *Phys. Rev. Lett.* **61**, 90 (1988)
 - [24] E. Esarey, P. Sprangle, J. Krall, and A. Ting, *IEEE Journal of Quantum Electronics* **33**, 1879 (1997)
 - [25] G. Li, PhD Thesis, University of Rochester (2012)
 - [26] D. Anderson and M. Bonnedal, *Phys. Fluids* **22**, 105 (1979)
 - [27] B. J. Duda and W. B. Mori, *Phys. Rev. E* **61**, 1925 (2000)

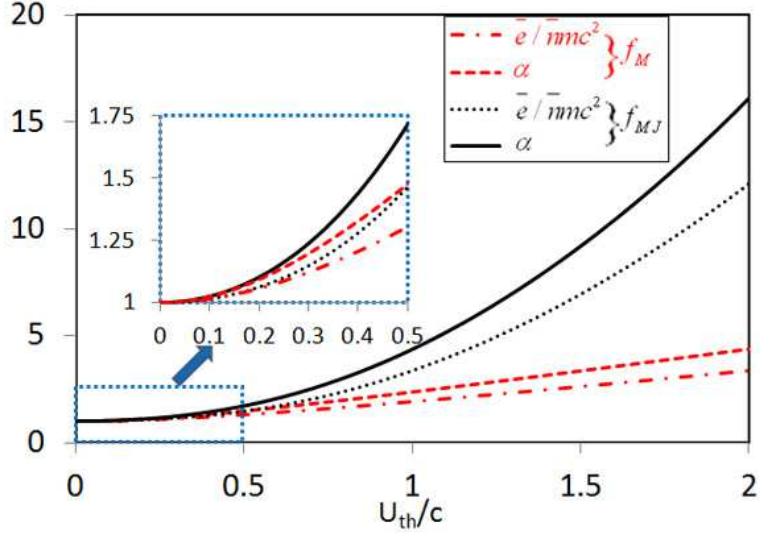


FIG. 1: (color online) A plot of the thermal parameter α vs. $U_{th}/c = \sqrt{T/mc^2}$ for two different distributions: Maxwellian (M) and Maxwell-Juttner (MJ).

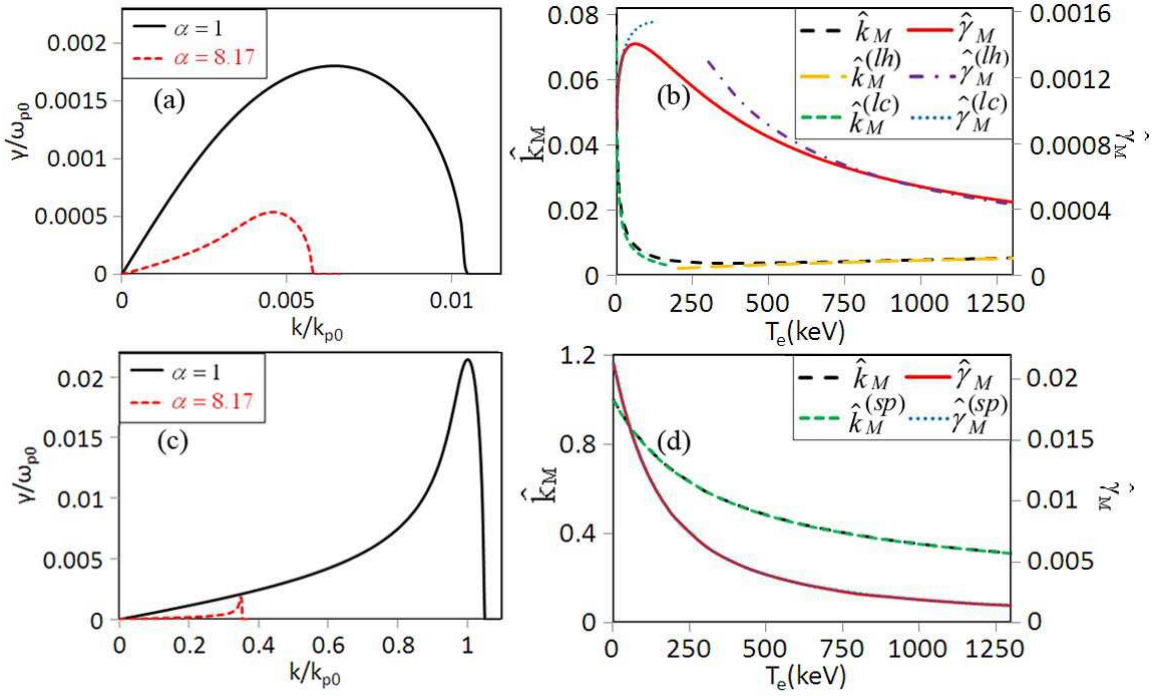


FIG. 2: (color online) Plots of typical growth rates vs. mode numbers [long pulses (a) and short pulses (c)] and the growth rates and mode numbers of the dominant modes vs. temperatures [long pulses (b) and short pulses (d)]

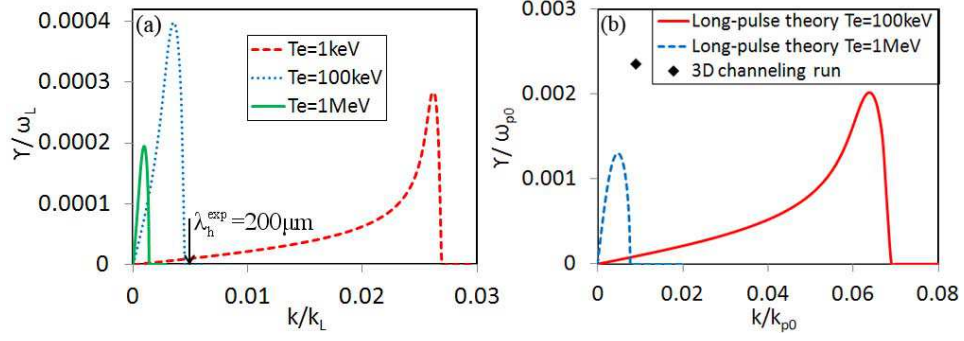


FIG. 3: (color online) Comparisons of the dominant mode number observed in the experiment[15] (a) and the simulation[7] (b) with those predicted by the long pulse theory.